AJNR

Intratumoral Microhemorrhages on T2*-Weighted Gradient-Echo Imaging Helps Differentiate Vestibular Schwannoma From Meningioma

K. Thamburaj, V.V. Radhakrishnan, B. Thomas, S. Nair and G. Menon

K. Thamburaj
V.V. Radhakrishnan
B. Thomas
S. Nair
G. Menon

Intratumoral Microhemorrhages on T2*-Weighted Gradient-Echo Imaging Helps Differentiate Vestibular Schwannoma From Meningioma

BACKGROUND AND PURPOSE: Vestibular schwannomas (VS) may be difficult to differentiate from cerebellopontine angle (CPA) meningiomas. Demonstration of microhemorrhages in VS on T2*-weighted gradient-echo (GRE) sequences may have potential value to differentiate VS from CPA meningiomas.

MATERIALS AND METHODS: In this prospective study of 20 patients, MR imaging was performed with T2*-weighted GRE in addition to all basic sequences. Histopathologic examination was performed after surgery. Intratumoral hemosiderin was confirmed by pigment staining.

RESULTS: There were 15 patients in the VS group with 16 VS and 5 in the meningioma group with 5 posterior fossa meningiomas. Fourteen of the 16 VS and all 5 meningiomas were treated surgically and were confirmed on histopathologic examination. T2*-weighted GRE identified microhemorrhages on T2*-weighted sequence in 15 (93.75%) of the 16 VS. CT excluded calcification in all VS. T2-weighted turbo spin-echo (TSE) and fluid-attenuated inversion recovery (FLAIR) images recognized microhemorrhages in 2 cases. Pigment staining confirmed hemosiderin in all 14 surgically treated VS, and none of the meningiomas showed microhemorrhages on MR imaging. For the detection of microhemorrhages, T2*-weighted GRE showed a sensitivity of 93.8%, specificity of 100%, positive predictive value of 100%, and negative predictive value of 83.3%. The sensitivity of T2 TSE and FLAIR for microhemorrhage was 12.5%. The Fisher exact test showed a statistically significant difference in the differentiation of VS from meningioma on the basis of detection of microhemorrhages ($P < .01$).

CONCLUSION: Most VS demonstrate microhemorrhages on T2*-weighted GRE. This finding is useful to differentiate VS from CPA meningiomas. T2*-weighted GRE should be used as a basic sequence to evaluate CPA tumors. Identification of microhemorrhages may have the potential to assess the aggressive biologic behavior of VS.

Vestibular schwannomas (VS) and meningiomas comprise most cerebellopontine angle (CPA) tumors. VS constitute 80% to 90% and meningiomas 10% to 15% of CPA tumors.[1] It is essential to distinguish these 2 lesions accurately before surgery because the outcome with preservation of hearing is better with meningiomas.[1] MR imaging is considered the imaging method of choice to assess CPA tumors and to distinguish VS from meningiomas. A tumor in the internal auditory canal (IAC) with dilation of the canal is highly suggestive of VS. Signs such as the presence of hyperostosis, calcification, broad base of the tumor against the tentorium, and a dural tail may favor the diagnosis of a meningioma.[2] However, both VS and meningioma may show similar imaging features, and hence it is not surprising that approximately 25% of CPA meningiomas are mistaken for VS.[3] Identification of microhemorrhages may be of interest to assess its relationship to the development of cystic changes in VS and to identify cases at risk of developing clinically significant intratumoral bleed. To our knowledge, no previous study has been done with T2*-weighted gradient-echo (GRE) sequence to assess the presence of intratumoral microhemorrhages and its diagnostic potential in identifying VS.

Methods

In our prospective study from March 2005 to September 2005, we included 20 patients. There were 15 patients in the VS group and 5 in the meningioma group. Because ours is a tertiary referral center, all patients already had undergone CT scan of the head before referral to undergo surgery. CT excluded intratumoral calcification in all VS and in 4 of the 5 meningiomas. Before MR imaging, we obtained informed consent in all patients. MR imaging of the brain was performed with a 1.5T system (Avanto; Siemens, Erlangen, Germany) with a phased array head matrix coil. We performed this imaging with a T2-weighted turbo spin-echo (TSE) sequence in the sagittal (TR, 4000 ms; TE, 112 ms; echo-train length (ETL), 13; number of acquisitions, 1) and axial planes (TR, 3010 ms; TE, 82 ms; ETL, 5; acquisition, 1), T1-weighted spin-echo (SE) in the axial plane (TR, 476 ms; TE, 11 ms; acquisitions 1), fast fluid-attenuated inversion recovery (FLAIR) in the axial plane (TI, 2500 ms; TR, 9000 ms; TE, 109 ms; acquisition, 1), T2*-weighted GRE in the axial plane (TR, 800 ms; TE, 26 ms; flip angle, 12°; acquisition, 1), and postgadolinium T1-weighted SE in all 3 orthogonal planes (TR, 550 or 805 ms; /TE, 11 ms; acquisition, 1). A section thickness of 5 mm was used in all 3 planes with an intersection gap of 0.5 to 1 mm. An image matrix of 374 × 512 and FOV of 220 × 240 mm were used. The presence of intratumoral microhemorrhages and hemosiderin staining of the cisterns and sulci were assessed in all sequences. Intratumoral microhemorrhages were identified as hypointense dots on MR imaging similar to the one described for cerebral microhemorrhages.[4] We counted the number of hypointense dots in each tumor on MR imaging visually and measured the size of each hypointense dot with an electronic caliper.

Histopathologic confirmation of the diagnosis was obtained in 14

Table 1: VS group

Patient No.	Age/Sex	Location	Size (cm) T x C x A	Consistency	No. of MH	Size of MH (mm)	Fluid Level	IAC Component	Sequence Showing MH Other Than T2*	Surgical Treatment	Pigment
1	52/M	R	$3.22 \times 3.41 \times 2.88$	S	9	<3	N	+	N	Y	Y
2	42/M	L	$3.77 \times 3.78 \times 4.21$	S	>40	5	N	+	T2 & FLAIR	Y	Y
3	41/F	R	$3.03 \times 3.57 \times 4.14$	S	17	2	N	+	N	Y	Y
4	36/F	R	$2.63 \times 2.95 \times 3.55$	S	14	4	N	+	N	Y	Y
5	30/M	L	$3.23 \times 3.48 \times 3.55$	S	6	5	N	+	N	Y	Y
6	60/F	R	$2.82 \times 3.1 \times 3$	S	5	2	N	+	N	Y	Y
7	59/F	R	$3.61 \times 2.43 \times 2.95$	S	>50	4	N	+	N	Y	Y
8	38/F	B/L	$4.02 \times 3.95 \times 4.67$ (R)	S	>50	5	N	+	N	Y	Y
			$2.73 \times 2.52 \times 3.32$ (L)	S	5	2	N	+	N	N	N
9	52/M	R	$1.45 \times 1.12 \times 1.12$	S	N	N	N	+	N	N	N
10	34/M	R	$3.68 \times N \times 2.88$	S	28	5	N	+	N	Y	Y
11	51/M	R	$3.09 \times 4.38 \times 4.88$	C	4	7	Y	+	T2 & FLAIR	Y	Y
12	23/F	R	$3.27 \times 4.73 \times 3.08$	S	6	4	N	+	N	Y	Y
13	36/M	R	$4.40 \times 4.20 \times 4.03$	S	10	4	N	+	N	Y	Y
14	22/M	R	$3.81 \times 4.73 \times 3.71$	S	69	5	N	+	N	Y	Y
15	18/M	R	$5.2 \times 6.09 \times 6.37$	S	140	8	Y	+	N	Y	Y

Note:—M indicates male; F, female; R, right; L, left; B/L, bilateral; S, solid; C, cystic (in Consistency column); N, no; Y, yes; MH, microhemorrhage; IAC, internal auditory canal; T, transverse; C, craniocaudal; A, anteroposterior; FLAIR, fluid-attenuated inversion recovery; +, present.

Table 2: Meningioma group

Patient No.	Age/Sex	Location	Size (cm) T × C × A	Consistency	No. of MH	Size of MH (mm)	Fluid Level	IAC Component	MH in IAC	Sequence Showing MH Other Than T2*	Surgical Treatment
1	59/F	CPA	$2.03 \times 2.69 \times 2.79$	S	N	N	N	N	N	N	Y
2	47/F	Tentorium	$4.55 \times 5.64 \times 4.97$	S	N	N	N	N	N	N	Y
3	44/F	Falcotentorial	$2.64 \times 3.33 \times 2.98$	S	N	N	N	N	N	N	Y
4	48/F	CPA	$2.22 \times 3.54 \times 3.32$	S	N	N	N	N	N	N	Y
5	44/M	CPA	$3.32 \times 3.16 \times 4.92$	S	N	N	N	+	N	N	Y

Note:—M indicates male; F, female; S, solid; N, no; Y, yes; MH, microhemorrhage; IAC, internal auditory canal; T, transverse; C, craniocaudal; A, anteroposterior; CPA, cerebellopontine angle; +, present.

VS and in all 5 meningiomas. Pigmentation study was carried out in all cases of surgically treated VS to identify hemosiderin. We did not perform pigmentation staining in meningiomas because they did not show microhemorrhages in MR imaging. A thickness of 3 to 4 μm was obtained from specimens and then embedded in paraffin. Deparaffinization followed by rehydration with phosphate-buffered saline was performed before postfixation with sodium citrate solution. Hematoxylin-eosin (H&E) staining was performed. We assessed the presence of hemosiderin pigment with Perl's stain using standard protocol. Slides were examined under a low- and high-power field microscope. We performed data entry with Excel spreadsheets and data analysis using SPSS, version 14.0 (SPSS, Chicago, Ill). The Fisher exact test (nonparametric) was used to calculate the measure of association. A P value of less than .05 was considered to indicate a statistically significant difference.

Results

Of the 15 patients in the VS group, 6 were women and 9 were men. Of the 5 patients in the meningioma group, there were 4 women and 1 man. The age range was 18 to 60 years (mean, 39.5 ± 12.8 years) in the VS group and 44 to 59 years (mean, 48.4 ± 6.2 years) in the meningioma group. In 15 patients in the VS group, there were 16 VS. One patient had neurofibromatosis type 2 (NF2) with bilateral VS and supratentorial meningiomas. In the meningioma group, 3 tumors were located in the CPA region, a fourth in the falcotentorial junction, and a fifth from the tentorium. Of the 16 VS, 13 were located on the right side and the rest on the left side. The imaging characteristics of the VS group are given in Table 1 and those of the meningioma group in Table 2. The size of the VS ranged from 1.45 to 6.37 cm (mean, 3.98 ± 1.06 cm). Of the 16 VS, 15 measured larger than 3 cm in maximum diameter. All VS showed intracanalicular extension.

Microhemorrhages were identified on T2*-weighted GRE sequence in 15 VS (Fig 1). A fluid level was observed in 2 (12.5%) cases of VS. One was a large multiloculated cystic schwannoma. Hemosiderin staining of the cyst wall was evident in this case. The second case with a fluid level showed a very small cyst measuring less than 10 mm, and the fluid level was evident only on T2*-weighted sequence. Similar to the observation in the case with large cysts, we noted hemosiderin staining of the cyst wall in this case as well. This tumor showed more than 140 microhemorrhages in total, the maximum of all VS studied. Although all VS in our study had an intracanalicular component, susceptibility artifacts at the bone-brain interface obscured assessment of the intracanalicular components and, consequently, microhemorrhages in 10 tumors. Of the remaining 6 tumors, we were able to identify microhemorrhages in the intracanalicular components in 4 tumors. The only VS that failed to show microhemorrhage in our study was a small tumor with a predominant intracanalicular and a small cisternal component. One patient with NF2 and bilateral VS also had a left jugular foramen schwannoma in which microbleeds were clearly seen, though the tumor was lying almost completely in the bony canal. The size of the microhemorrhages in VS ranged from 2 to 8 mm in diameter (mean, $4.3 \pm$
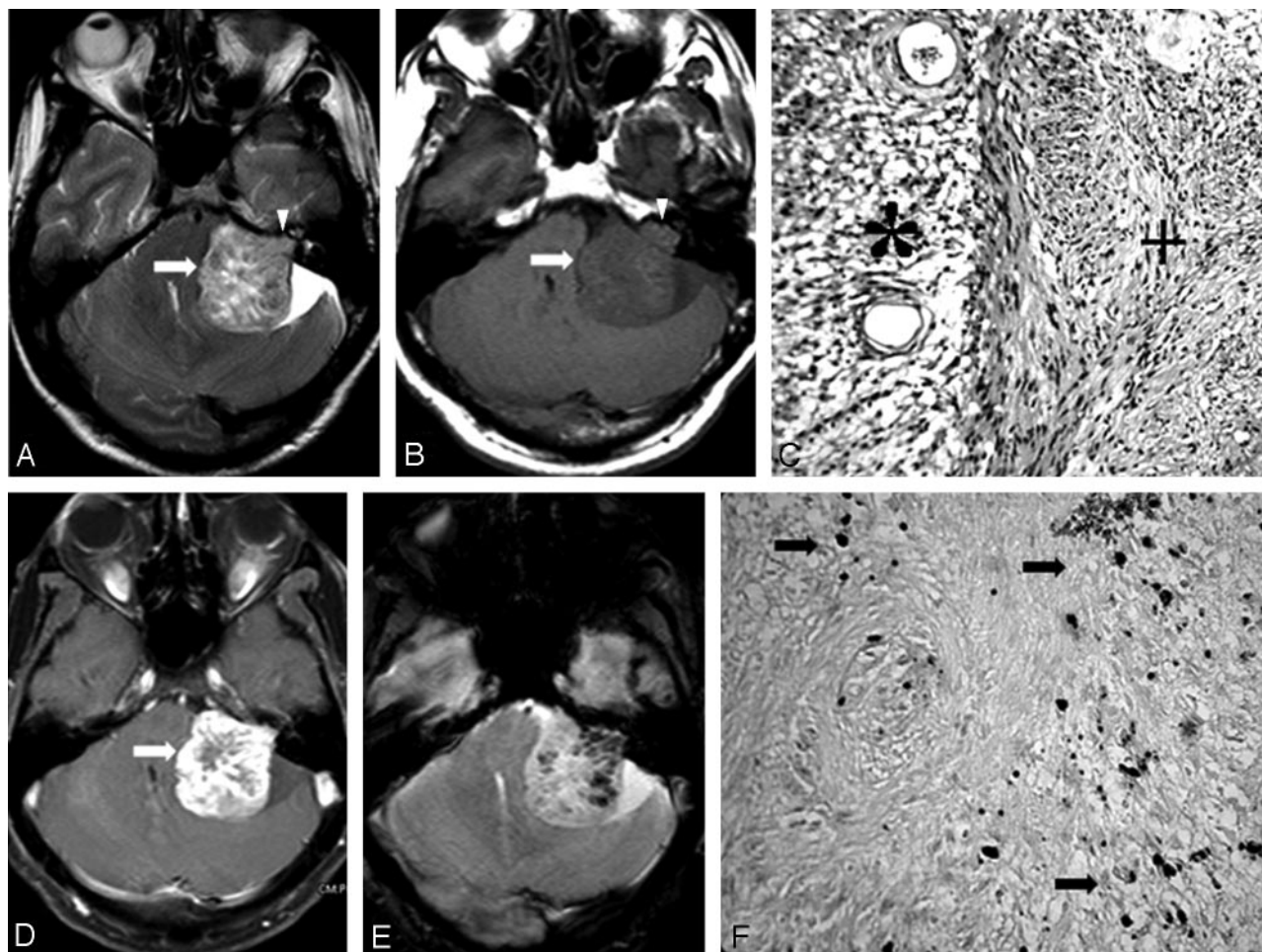
Fig 1. *A–B,* Axial T2- and T1-weighted images, respectively, of left VS show no evidence of hemorrhage (*arrow*). Note the extension into the IAC (*arrowhead*). *C,* Photomicrograph shows the Antoni A (+) and Antoni B (*) components in the VS (H&E ×150). *D,* Axial postcontrast T1-weighted image shows bright enhancement of the tumor with nonenhancing areas (*arrow*). *E,* T2*-weighted GRE shows multiple hypointense intratumoral signals suggestive of microhemorrhage. *F,* Photomicrograph showing discrete and confluent masses of hemosiderin pigments (*arrow*) in the Schwann cell tumor (Perls stain ×150).

1.8 mm). Each tumor showed multiple microhemorrhages ranging from 4 to 140 (mean, 30.4 ± 36.8). The 2 tumors with fluid levels were associated with the largest-sized microhemorrhages (7 and 8 mm). We did not observe hemosiderin staining of the tumor boundary, tumor-brain interface, or cisternal and sulcal spaces in any of these cases. The matrix of the tumor was heterogeneously hyperintense on T2-weighted TSE in 15 VS. One small VS showed homogeneous signal intensities. Apart from the T2*-weighted GRE sequence, we were able to identify microhemorrhage with T2-weighted TSE and FLAIR in 2 cases. In both these cases, the number of microhemorrhages did not exceed 2. Pigment staining confirmed the presence of hemosiderin in all 14 surgically treated tumors (Fig 1). Pigments were present in both Antoni A and B components. In addition, fresh hemorrhages and thrombosed vessels were recognized in all tumors.

Among the 5 cases of meningioma, IAC extension was observed in 1 case, though there was no dilation of the auditory canal (Fig 2). The dural tail was evident in 3 cases, the flat base against the dura or bone in 2 cases, and calcification in 1 case. The calcification appeared as clump-like, measuring 20 mm, and it could be easily distinguished from the typical dot-like appearance of microhemorrhages on T2*-weighted GRE se-
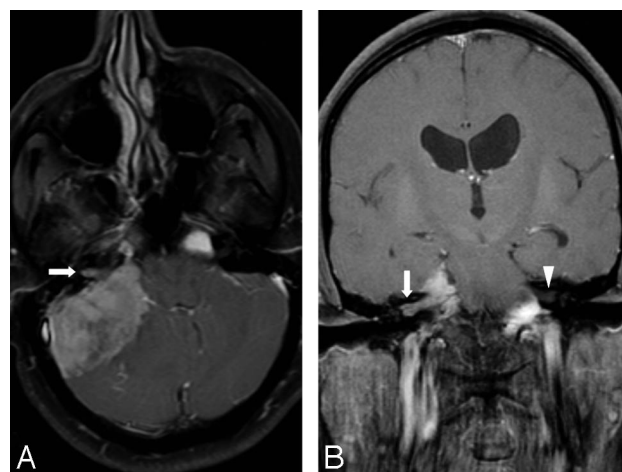

Fig 2. *A,* T1-weighted postgadolinium axial image shows right CPA meningioma with extension into the adjacent IAC (*arrow*). *B,* T1-weighted postgadolinium coronal image shows extension of the tumor into the IAC more clearly (*arrow*) compared with the contralateral IAC (*arrowhead*).

quence. We observed similar findings in the 2 supratentorial meningiomas in the patient with NF2. The size of the meningiomas varied from 2.79 to 5.64 cm (mean, 3.97 ± 1.25 cm).
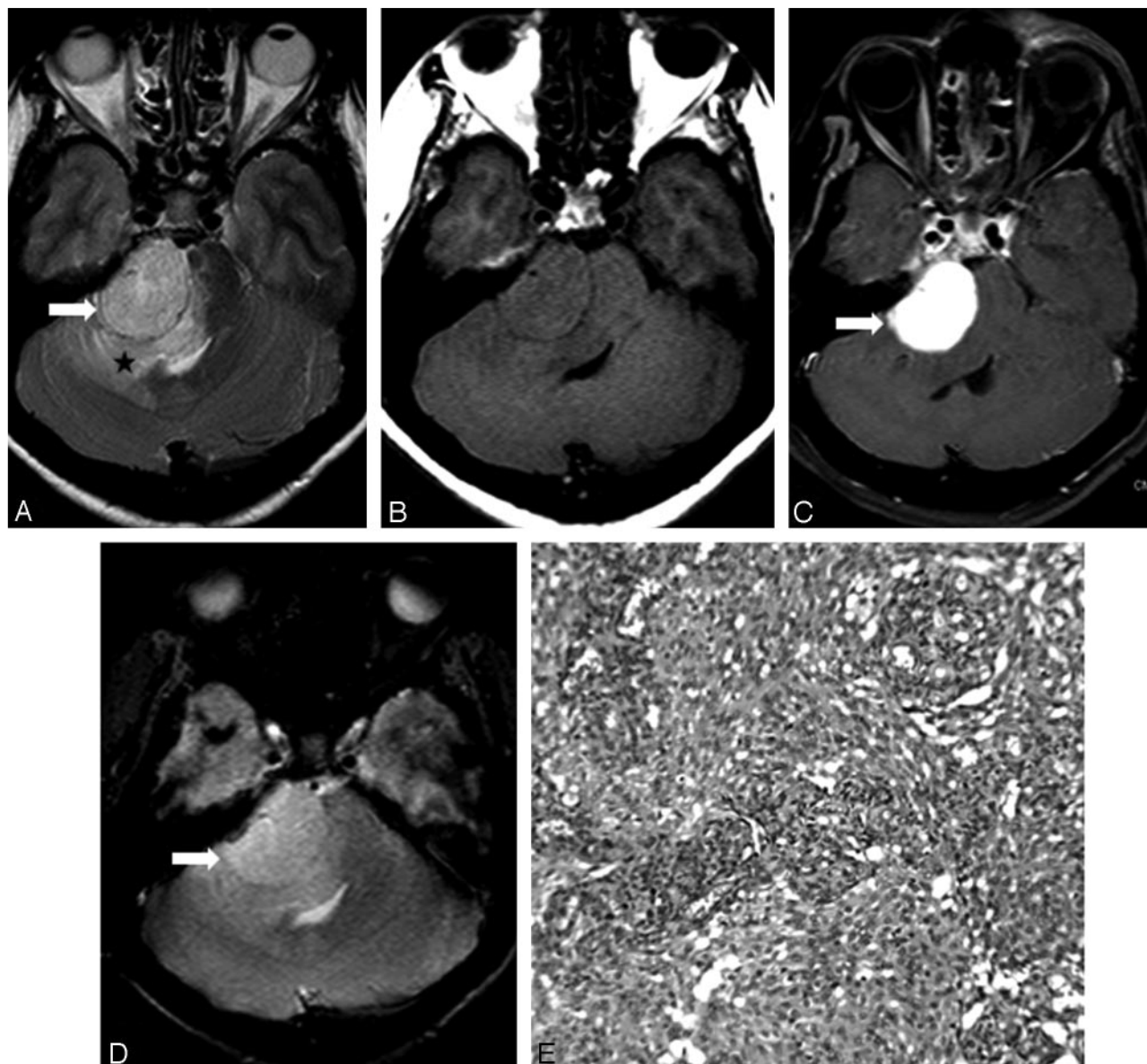
Fig 3. *A,* Axial T2-weighted TSE image shows the relatively hyperintense meningioma in the right CPA with a broad base against the petrous bone (*arrow*). Note the vasogenic edema of the adjacent cerebellum and middle cerebellar peduncle (*star*). *B,* On axial T1-weighted SE, the tumor is isointense to the brain. *C,* Postcontrast T1-weighted image at the corresponding level shows intense enhancement of the tumor (*arrow*). *D,* Axial T2*-weighted GRE does not show hypointense signals characteristic of microhemorrhage in the tumor (*arrow*). The tumor matrix appears homogeneous. *E,* Photomicrograph showing features of a meningioma in which neoplastic cells are displayed in concentric whorls and lobules of varying sizes. These neoplastic cells are supported on a vascularized connective stroma (H&E ×150).

All meningiomas were solid without evidence of cystic changes or hemorrhage, and none showed microhemorrhages on T2*-weighted GRE sequence (Fig 3). Uniform enhancement was observed in all 5 cases.

Statistical analysis revealed a sensitivity of 93.8%, specificity of 100%, positive predictive value of 100%, and negative predictive value of 83.3% for T2*-weighted GRE sequence in identifying microhemorrhages in VS. The sensitivity of T2-weighted TSE and FLAIR was only 12.5%. The Fisher exact test was performed to assess the association of microhemorrhages in distinguishing VS from meningioma and showed a statistically significant difference ($P < .01$).

Discussion

CPA tumors constitute 8% to 10% of intracranial tumors.[5] The most common CPA tumors are VS, which make up 80%

to 90% of CPA tumors.[6] Compared with VS, meningiomas are the next most common CPA tumor constituting 10% to 15% of all CPA tumors.[1] The treatment and operative approach differ for VS and meningioma, and consequently an accurate preoperative diagnosis is warranted to distinguish these 2 tumors.[7] Meningiomas seem to offer better chances to preserve hearing than VS.[1,7] An accurate preoperative diagnosis may influence the prognosis because meningiomas are known to have a higher incidence of recurrence.[7] Multiplanar capability, superior soft tissue contrast resolution, and lack of beam hardening artifacts make MR imaging the preferred technique to assess CPA tumors.[6] Several helpful imaging signs on CT and MR imaging have been described in the literature to distinguish VS from CPA meningiomas. The globular shape of a tumor, canalicular component in association with dilation of the internal auditory canal, and formation of an acute angle by

the anterolateral or posterolateral tumor border with the adjacent petrous bone all suggest the possibility of a VS rather than a meningioma.[2,8] On the other hand, a sessile tumor with a broad base against petrous bone or tentorium, formation of an obtuse angle with the petrous temporal bone, homogeneous contrast enhancement, dural tail, intratumoral calcification, and hyperostotic changes all favor the diagnosis of a meningioma.[2,6,8-10] Excluding hyperostosis, no other sign is considered specific to meningioma.[2] Furthermore, the dural tail sign has been observed in association with VS.[11] Hence, it is not surprising that in a recent study, 25% of cases of CPA meningiomas were mistaken for VS.[3]

Intratumoral microhemorrhages identified on T2*-weighted GRE sequence in VS seem to hold diagnostic potential to distinguish VS from meningiomas. Of the 16 VS in our study, 15 demonstrated intratumoral microhemorrhages on the T2*-weighted GRE sequence, whereas none of the 5 posterior fossa meningiomas showed this finding. The ability of T2*-weighted GRE sequence to demonstrate hemosiderin and other breakdown products of hemoglobin is well established. It is considered to be one of the most sensitive MR sequences to demonstrate hemorrhage.[12] Autopsy studies have established the correlation between foci of hypointense signals on T2*-weighted GRE sequence and cerebral microhemorrhages.[4] The occurrence of microhemorrhages is a well-known pathologic feature of VS.[13] Although T2*-weighted GRE is regularly used to assess cerebral microhemorrhages, to the best of our knowledge, it has never been used to identify microhemorrhages in VS. The abnormal vascularity found in VS is considered responsible for the development of microhemorrhages.[13] From a histologic standpoint, the abnormal vascularity in VS is characterized by focal sinusoidal dilations, hyaline thickening of vascular walls, and cavernous or telangiectatic formation. These changes are thought to predispose to the development of spontaneous thrombosis, necrosis, and formation of microhemorrhages in the tumor.[13] Neoplastic Schwann cells themselves may show hemosiderin because of their phagocytic properties, similar to macrophages.[13] Although MR imaging is exquisitely sensitive for the detection of microhemorrhage, only a few MR studies in the literature have shown the presence of microhemorrhages in VS.[14,15] The major reason for this could be the use of the T2-weighted sequence, which is inherently less sensitive than the T2*-weighted GRE sequence in the identification of microhemorrhage in these studies.[16] By using T2-weighted sequence, Ishii et al[14] demonstrated microhemorrhages in 5 of 12 VS measuring more than 25 mm in diameter. Park et al[15] demonstrated microhemorrhage in 35% of VS in their study by using the T2-weighted sequence, though histopathologic examination revealed hemosiderin in all cases. In our study, T2*-weighted GRE images demonstrated microhemorrhages in 15 of 16 VS, resulting in a sensitivity of 93.8%, a specificity and positive predictive value of 100%, and a negative predictive value of 83.3% with T2*-weighted GRE sequences in the detection of microhemorrhages, whereas T2-weighted TSE and FLAIR sequences showed microhemorrhages in only 2 tumors, resulting in a sensitivity of 12.5%. The 180 refocusing pulse used with a T2-weighted sequence eliminates most of the susceptibility-induced phase incoherence from T2*-weighted effects. T2-weighted TSE or FSE shows less sensitivity in the detection

of microhemorrhages.[16] Hence, T2*-weighted GRE seems to be the best sequence to detect microhemorrhages in VS as shown in our study.

Meningiomas are known to be richly vascular tumors and may occasionally present with intratumoral, subarachnoid, or subdural hemorrhage, particularly with angioblastic and meningotheliomatous meningiomas.[13,17] Cystic changes in meningiomas have been associated with hemorrhage and aggressive behavior.[2] Focal concentrations of thin-walled vessels and endothelial channels have been recognized close to the gross bleeding sites in meningiomas. Arteriolar hyalinization has been also recognized in meningiomas presenting with hemorrhage.[18] Despite these known pathologic features of meningiomas, we did not observe intratumoral microhemorrhages on T2*-weighted GRE sequence in any of the 5 posterior fossa meningiomas in our study. Although our numbers are small, we have yet to observe microhemorrhages in any of the supratentorial meningiomas – one of the common intracranial tumors managed in our institute – despite using T2*-weighted GRE sequence on a regular basis. We are unable to offer a clear explanation for the lack of microhemorrhages in MR images in meningiomas. Perhaps meningiomas lack the exact microvascular changes observed in VS. Approximately 25% of meningiomas are known to exhibit calcification.[2] Calcification is typically observed as signal intensity void in T2*-weighted GRE image and may be mistaken for bleed.[19] In our study, although we observed calcification on CT in one of the posterior fossa meningiomas, it did not resemble the typical dot-like appearance of microhemorrhages on T2*. Furthermore, in the patient with NF2 in our study, calcification was observed in 2 supratentorial meningiomas, but they also did not resemble the appearance of microhemorrhages. Calcification in meningiomas may take the form of diffuse psammomatous-type, irregular, patchy calcification; ring calcification; nodular calcification; and solid calcification.[20] Although it is theoretically possible for multiple punctate calcifications to mimic the appearance of microhemorrhages on T2*-weighted GRE image, one should be able to exclude this possibility with a CT scan. The 3D susceptibility-weighted gradient sequence should offer an additional benefit in showing more microhemorrhages than T2*-weighted GRE.[21] Recently, we have introduced this sequence in our system and are able to identify consistently more hemosiderin deposits with this sequence than with T2*-weighted GRE.

Apart from offering a help in diagnosis, MR recognition of microhemorrhages may hold significance to assess the biologic behavior of VS. Recently, microhemorrhages have been thought to play a dominant role in the development of cystic changes in VS.[15] These cystic changes, in turn, may induce large intratumoral hemorrhage and, at times, subarachnoid hemorrhage with adverse outcome.[22,23] Misra et al[22] believe urgent surgery may be needed in cystic VS to avoid the risks for a large hemorrhage. Furthermore, smaller VS may be treated with either gamma knife surgery or conservative management, especially in patients older than 65 years. It is recommended that intervention be based on a combination of rapid tumor growth with development of symptoms.[24]

Previous studies[22,25] suggested the possibility of positive influence of the size of VS on the incidence of hemorrhage. Furthermore, Gomez-Brouchet et al[26] found a significant cor-

relation between the size of VS and hemosiderin deposits. We did not find any relationship between the size of the tumor and the number of intratumoral microhemorrhages in our study, though we observed the largest of the microhemorrhages in association with 2 VS with cyst and fluid levels. It may be interesting to address the relationship between fluid levels and the number of intratumoral microhemorrhages in a study with a large patient population. Furthermore, it may be of interest to know whether there is any relationship between the number of intratumoral microhemorrhages and clinical presentation as well as that of the biologic behavior of VS.

A drawback with the T2*-weighted GRE sequence in the demonstration of microhemorrhages is its tendency to exaggerate bone-brain boundary artifacts.[19] This is perhaps responsible for the failure to demonstrate microhemorrhages in the only case of a patient with VS in our study. In this patient, the tumor measured 1.45 cm in diameter with a predominant canalicular component. Artifacts from the bone-brain interface obscured the visualization of the canalicular component as well as the small cisternal component and, thus, intratumoral microhemorrhages. Because of the small size of the tumor, the patient did not undergo surgery. However, it seems that bone-boundary artifacts need not interfere with demonstration of microhemorrhages in each case of an intracanalicular component. In at least 4 tumors, we observed clearly the intracanalicular component with microhemorrhages on T2*-weighted GRE sequence. Furthermore, 2 other VS clearly showed the intracanalicular component without microhemorrhages on T2*.

The major drawback of our study was the small patient population. This may have been addressed if a study were carried out to assess all intracranial meningiomas with either T2*-weighted GRE sequence or the latest 3D susceptibility-weighted sequence. We recently introduced this 3D susceptibility-weighted sequence and found consistently more microhemorrhages demonstrated than on the conventional T2*-weighted GRE.

Conclusion

MR imaging demonstrates microhemorrhages in most VS. This feature is useful to differentiate VS from CPA meningiomas. Microhemorrhages can be shown best by either T2*-weighted GRE sequence or the latest and more sensitive 3D susceptibility-weighted sequence. Identification of microhemorrhages may have the potential to address aggressive biologic behavior of VS and thus may influence the course of management.

References

1. Nakamura M, Roser F, Dormiani M, et al. **Facial and cochlear nerve function after surgery of cerebellopontine angle meningiomas**. *Neurosurgery* 2005;57: 77–90; discussion 77–90
2. Tong KA, Harnsberger HR, Swartz JD. **The vestibulocochlear nerve, emphasizing the normal and diseased internal auditory canal and cerebellopontine angle**. In: Swartz JD, Harnsberger HR, eds. *Imaging of the Temporal Bone*, 3rd ed. New York: Thieme; 1998:394–472
3. Grey PL, Moffat DA, Hardy DG. **Surgical results in unusual cerebellopontine angle tumours**. *Clin Otolaryngol Allied Sci* 1996;21:237–43
4. Fazekas F, Kleinert R, Roob G, et al. **Histopathologic analysis of foci of signal loss on gradient-echo T2*-weighted MR images in patients with spontaneous intracerebral hemorrhage: evidence of microangiopathy-related microbleeds**. *AJNR Am J Neuroradiol* 1999;20:637–42
5. Mallucci CL, Ward V, Carney AS, et al. **Clinical features and outcomes in patients with non-acoustic cerebellopontine angle tumours**. *J Neurol Neurosurg Psychiatry* 1999;66:768–71
6. Zamani AA. **Cerebellopontine angle tumors: role of magnetic resonance imaging**. *Top Magn Reson Imaging* 2000;11:98–107
7. Voss NF, Vrionis FD, Heilman CB, et al. **Meningiomas of the cerebellopontine angle**. *Surg Neurol* 2000;53:439–46; discussion 446–47
8. Lalwani AK, Jackler RK. **Preoperative differentiation between meningioma of the cerebellopontine angle and acoustic neuroma using MRI**. *Otolaryngol Head Neck Surg* 1993;109:88–95
9. Ryoo JW, Na DG, Woo JY, et al. **Investigation of juxtasellar and cerebellopontine angle meningiomas and neurogenic tumours: two-phase helical CT**. *Neuroradiology* 2001;43:637–43
10. Mikhael MA, Ciric IS, Wolff AP. **Differentiation of cerebellopontine angle neuromas and meningiomas with MR imaging**. *J Comput Assist Tomogr* 1985;9:852–56
11. Paz-Fumagalli R, Daniels DL, Millen SJ, et al. **Dural "tail" associated with an acoustic schwannoma in MR imaging with gadopentetate dimeglumine**. *AJNR Am J Neuroradiol* 1991;12:1206
12. Hayman LA, Taber KH, Ford JJ, et al. **Mechanisms of MR signal alteration by acute intracerebral blood: old concepts and new theories**. *AJNR Am J Neuroradiol* 1991;12:899–907
13. Urich H, Tien RD. **Tumors of the cranial, spinal and peripheral nerve sheaths**. In: Bigner DD, McLenden RE, Bruner JM, eds. *Russell and Rubinstein's Pathology of Tumors of the Nervous System, Vol. 2*, 6th ed. London: Arnold; 1998:141–93
14. Ishii K, Takahashi S, Matsumoto K, et al. **Hemorrhage and abnormal veins in acoustic neurinoma: MR findings**. *Radiat Med* 1996;14:65–69
15. Park CK, Kim DC, Park SH, et al. **Microhemorrhage, a possible mechanism for cyst formation in vestibular schwannomas**. *J Neurosurg* 2006;105:576–80
16. Krishnamoorthy T, Fiorelli M. **MR detection of intracranial hemorrhage**. In: von Kummer R, Back T, eds. *Magnetic Resonance Imaging in Ischemic Stroke*. Berlin: Springer; 2006:159–70
17. Zee CS, Chen T, Hinton DR, et al. **Magnetic resonance imaging of cystic meningiomas and its surgical implications**. *Neurosurgery* 1995;36:482–88
18. Russell EJ, George AE, Kricheff II, et al. **Atypical computed tomography features of intracranial meningioma: radiological-pathological correlation in a series of 131 consecutive cases**. *Radiology* 1980;135:673–82
19. Atlas SW, Grossman RI, Hackney DB, et al. **Calcified intracranial lesions: detection with gradient-echo-acquisition rapid MR imaging**. *AJR Am J Roentgenol* 1988;150:1383–89
20. New PF, Aronow S, Hesselink JR. **National Cancer Institute study: evaluation of computed tomography in the diagnosis of intracranial neoplasms. IV. Meningiomas**. *Radiology* 1980;136:665–75
21. Wycliffe ND, Choe J, Holshouser B, et al. **Reliability in detection of hemorrhage in acute stroke by a new three-dimensional gradient recalled echo susceptibility-weighted imaging technique compared to computed tomography: a retrospective study**. *J Magn Reson Imaging* 2004;20:372–77
22. Misra BK, Rout D, Bhiladvala DB, et al. **Spontaneous haemorrhage in acoustic neurinomas**. *Br J Neurosurg* 1995;9:219–21
23. Sugihara S, Kinoshita T, Matsusue E, et al. **Multicystic acoustic schwannoma with intratumoral hemorrhage: a report of two cases**. *Magn Reson Med Sci* 2004;15:101–04
24. Rosenberg SI. **Natural history of acoustic neuromas**. *Laryngoscope* 2000;110:497–508
25. Odabasi AO, Buchman CA, Morcos JJ. **Tumor-associated hemorrhage in patients with acoustic neuroma**. *Am J Otol* 2000;21:706–11
26. Gomez-Brouchet A, Delisle MB, Cognard C, et al. **Vestibular schwannomas: correlations between magnetic resonance imaging and histopathologic appearance**. *Otol Neurotol* 2001;22:79–86